Journal of Genetic Engineering and Biotechnology (2011) 9, 77–82

Academy of Scientific Research & Technology and
National Research Center, Egypt

Journal of Genetic Engineering and Biotechnology

www.elsevier.com/locate/jgeb

ARTICLE

A three dimensional finite element study on dental implant design

Mohamed I. El-Anwar [a], Mohamed M. El-Zawahry [b,*]

[a] *Mechanical Engineering Department, National Research Centre, Egypt*
[b] *Prosthodontics Department, National Research Centre, Egypt*

Received 10 May 2011; accepted 10 May 2011
Available online 21 June 2011

KEYWORDS

Dental implant;
Design;
FEM;
Prosthodontics

Abstract Implant diameter and length are the most effective parameters affecting stress distribution in surrounding bones. In order to extract simplified design equations to better understand implants behavior, 25 different implant designs with gradual increase in diameter and length were analyzed in 3D using Finite Element Method. Four types of loadings were applied on each design: tension of 50 N, compression of 100 N, bending of 20 N, and torque of 2 Nm to derive design curves.

Analysis of results showed that increasing implant diameter and length generate better stress distribution on spongy and cortical bones. Approximate design equations and curves were obtained as a result of this study.

1. Introduction

The relation between implant design and load distribution at the implant bone interface is an important issue to understand [22].

Many factors affect load transfer at the bone implant interface such as the type of loading, material properties of the implant and prosthesis, implant geometry, surface structure, implant design quality (diameter and length) and quantity of surrounding bone, and nature of bone implant interface [12]. Cylindrical implant type was investigated in this study as illustrated in (Fig. 1).

One consequence of jawbone atrophy may be that no bone is present in the jaw areas where teeth are to be placed. This is problematic for the implantologist and leads to the preference of performing bone augmentation.

Basal implants overcome such problem in a manner that is different than that of cylindrical ones. Their baseplates are anchored in small, native bone areas which are often far from the actual clinical tooth, i.e. distant in a vertical/sagittal and/or horizontal direction. Although clinical experience has led to the development of a variety of basal implant designs, the surgical situation may demand variable positioning of the

* Corresponding author.
E-mail address: mohamed_zawahry@yahoo.com (M.M. El-Zawahry).

1687-157X © 2011 Academy of Scientific Research and Technology. Production and hosting by Elsevier B.V. All rights reserved.

Peer review under National Research Center, Egypt.
doi:10.1016/j.jgeb.2011.05.007

Production and hosting by Elsevier

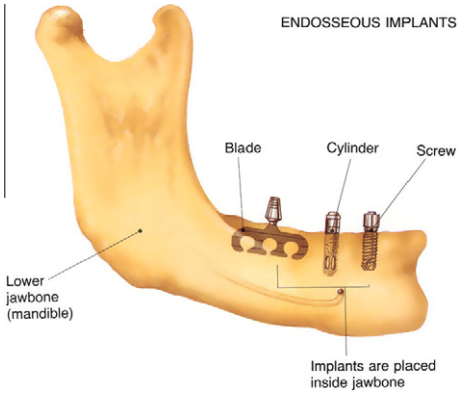

Figure 1 Implant types [13].

interconnection implant part (screw hole or cementing post). For this reason, the surgeon has to bend the vertical part of the implant before or after the insertion in order to allow easy prosthetic access of the connection area [26].

Twenty-five models have been developed in this study taking into account the following:

- Gradual increase in implant diameter.
- Gradual increase in implant length.
- The use of the plain implant type (model without threads).
- The process of modeling and loading on inserted implant is assumed to be harmless to the bone if the resulting forces on the bone interface remain within the range of its elastic deformation (creating no or only a limited number of cracks or micro-cracks).
- The forces must be within a range that can be applied by the surgeon inside the oral cavity.

In previous articles, models were created to describe the interaction between bone and basal implants using finite element analysis. A novel approach for modeling different interactions between cortical and cancellous bone was proposed [17,18]. This approach has been used for describing different stages of osseointegration and remineralization. In daily clinical practice during previous computations, the problem of stress distribution within dental implant bodies undergoing intra-operative bending vs. implant bodies machined in angulated designs out of one piece of metal became of interest.

The use of Finite Element Method (FEM) in the mechanical analysis of dental implants has been described by many authors such as Satoh et al. [24], Çaglar et al. [3], El-Anwar [9] and El-Zawahry et al. [10]. This method, presents suitable degree of reliability and accuracy [12,13] "without the risk and expense of implantation" [6]. To study a complex mechanical problem, FEM can be used to simulate and analyze stress distribution, dividing the 3D problematic geometry into a collection of very small elements. Image data obtained with the aid of computed tomography, 3-D scanner or magnetic resonance imaging is used to generate the FEM model and the mesh necessary for the analysis. The resulting models consist of elements, nodes and predefined boundary conditions. Displacement and stresses caused by loading can be calculated by computer packages at each node [27].

2. Materials and methods

The understanding of dental implant mechanical behavior during loading process comes from clinical practice findings, where the problem of the durability prediction during implantation procedure arises. A set of finite element models describing possible different applied forces formed at implantation were chosen as a suitable method.

The geometric model generation in this study was based on previous works with the development of a model of implants fixed to an edentulous mandible [7,8].

Bone geometry was simplified and simulated as a cylinder that consists of two co-axial cylinders. The inner one represents the spongy bone (diameter 14 mm and height 22 mm) that fills the internal space of the other cylinder (shell of 1 mm thickness) that represents the cortical bone (diameter 16 mm and height 24 mm). The 25 different implant designs used in this study cover the diameter range from 3.5 to 6.0 mm and length range from 9.0 to 13.0 mm. Plain implant is simply modeled by a cylinder with removed part (0.5 mm thickness). Each implant was subjected to four different loading conditions: tension at 50 N, compression at 100 N, bending at 20 N and torque at 2 Nm. The base of the finite element models are set to be fixed which defined the boundary condition [25]. Loading was applied on the top middle node of each implant assembly in the studied models. Torque was generated by using two equal forces in magnitude, opposite in direction, applied to two opposite points on the diameter of the implant head.

Linear static analysis was performed. The solid modeling and finite element analysis were performed on a personal computer Intel Pentium IV, processor 2.8 GHz, 1.0 GB RAM. The meshing software was ANSYS version 9.0 and the used element in meshing all three-dimensional models is eight nodes Brick element (SOLID45), which has three degrees of freedom (translations in the global directions) [19]. Mesh density is another relevant parameter. As the geometries are curved, improving the mesh has the usual effect of improving the results for the discrete model (increasing the accuracy of the obtained stress levels in regions of high stress gradients). Another effect of increasing the number of elements is the reduction of sharp angles that are artificially created through the geometric model substitution process (by the mesh), thus reducing artificial peak stresses through the improvement of actual geometry representation.

Table 1 lists the number of nodes and elements of the 25 models with indication to the implant model geometry type. The material properties used in this study are listed in Table 2.

Deep analysis correlating implant length, diameter, cross-sectional area to side area, and design curves were obtained from this study. This analysis may help in selecting the suitable implant geometry to be used with patient jaw-bone conditions and limit of stresses can be withstand.

3. Results

Four runs on each of the 25 models were done, simulating the four loading conditions prescribed for this study. Preference was for graphical comparisons due to the large number of models and load cases; while tabling and curve fitting using

Table 1 Twenty-five models (dimensions, number of nodes and elements).

Model #	Diameter (mm)	Length (mm)	No. of nodes	No. of elements
1	3.5	9	10,468	58,036
2		10	11,606	64,471
3		11	12,146	67,470
4		12	12,753	70,805
5	3.5	13	13,177	73,077
6	4.0	9	9676	53,621
7		10	10,469	57,969
8		11	11,412	63,285
9		12	12,120	67,244
10	4.0	13	11,856	65,517
11	4.5	9	9092	50,330
12		10	11,340	63,529
13		11	12,156	68,067
14		12	11,521	63,786
15	4.5	13	10,954	60,364
16	5.0	9	7925	43,694
17		10	10,188	57,039
18		11	8661	47,546
19		12	9424	51,871
20	5.0	13	10,672	59,052
21	6.0	9	6788	37,242
22		10	7143	39,135
23		11	7636	41,875
24		12	8121	44,412
25	6.0	13	8678	47,569

Table 2 Material properties.

	Young's modulus (MPa)	Poisson's ratio, ν
Cortical bone	1340	0.30
Spongy bone	150	0.30
Implant (titanium)	110,000 (per ASTM E8-04)	0.35

Least Squares Method to obtain results may lead to design equations and curves.

Analyses of Figs. 2–9, which summarize the results of this study, can guide to helpful and powerful design curves and

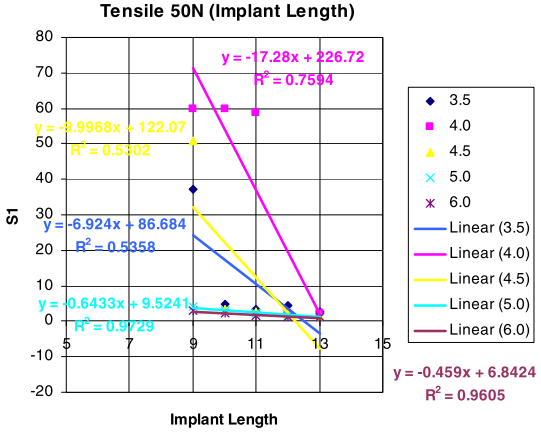

Figure 2 Maximum tensile stress in cortical bone under 50 N tension loading.

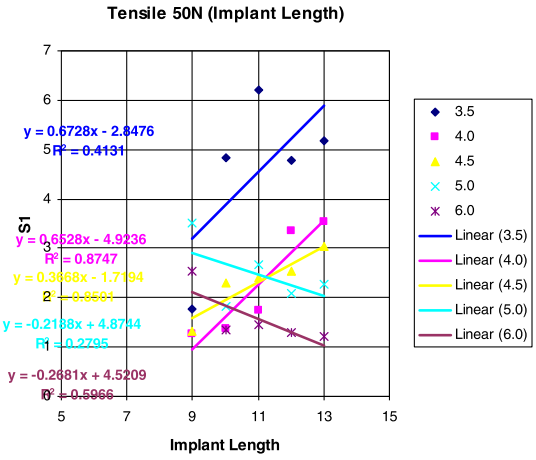

Figure 3 Maximum tensile in spongy bone under 50 N tension loading.

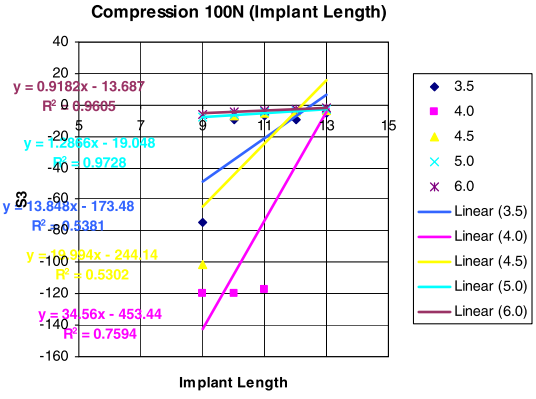

Figure 4 Maximum compression in cortical bone under 100 N compression loading.

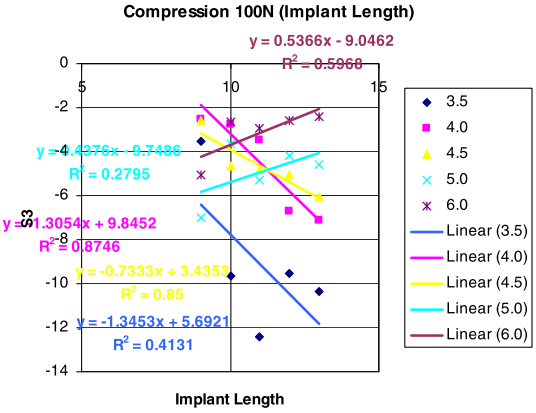

Figure 5 Maximum compression in spongy bone under 100 N compression loading.

equations. Trend lines and/or curve fitting are fairly enough for extracting the required data. Increasing implant length for small implant diameters dramatically reduces the values of generated stresses on cortical bone. In other words,

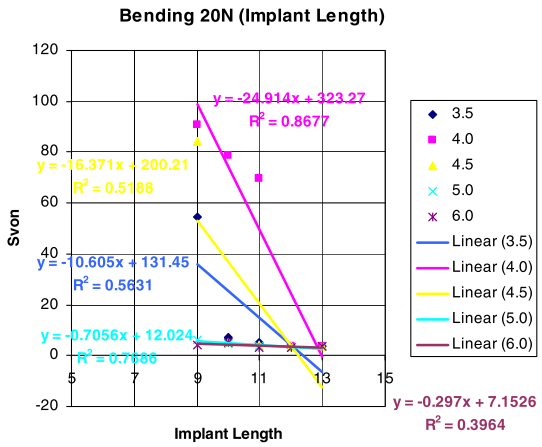

Figure 6 Von Mises in cortical bone under 20 N bending loading.

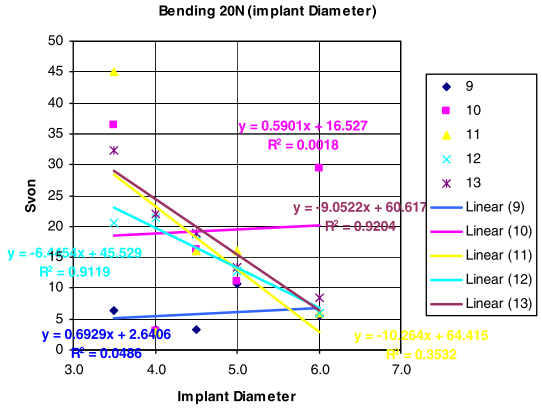

Figure 7 Von Mises in spongy bone under 20 N bending loading.

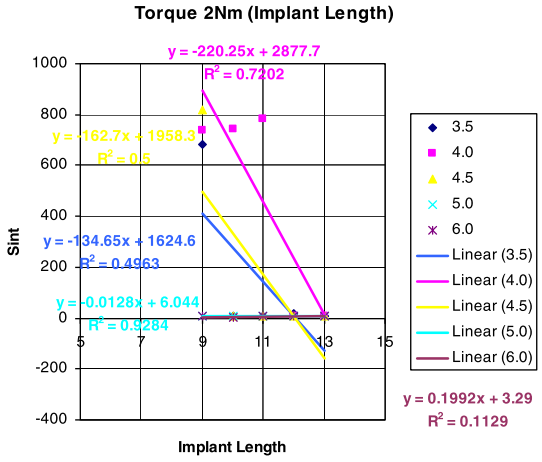

Figure 8 Stress intensity in cortical bone under 2 Nm torque loading.

increasing side area for implants with small diameters reduces the generated stresses on cortical bone. Side area can also be

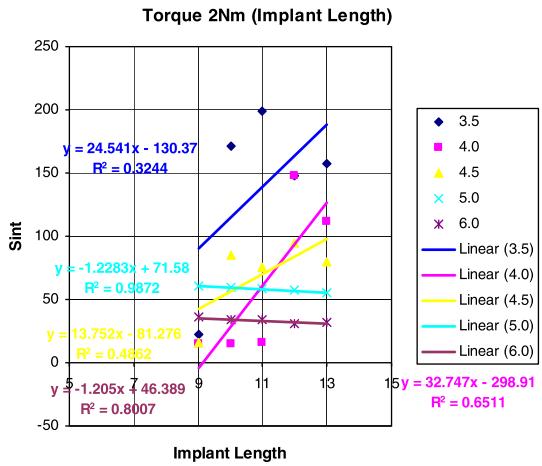

Figure 9 Stress intensity in spongy bone under 2 Nm torque loading.

increased by adding threads and micro-threads, changing thread, etc. type.

On the contrary, spongy bone received more energy by increasing implant length, which resulted in higher level of generated stresses.

For short implants, increasing diameter improves its effect on cortical bone (as it reduces generated stresses). In these cases, both side and cross-sectional areas were increased. The ratio of side to cross-sectional area is $4 \times$ length/diameter, i.e. increasing diameter reduces the ratio between side and cross-sectional areas. Comparing stress values on cortical bone while side area and cross-sectional area increase revealed a reduction in cortical bone stress values by increasing side area.

As an example, Fig. 10 showing a sample of the obtained results from model No. 25 under compressive loading of 50 N.

4. Discussion

The purpose of this investigation was to provide an analysis among different geometric configurations of implants and to compare their biomechanical behavior. Model results can be very close to the actual situation observed in clinical studies even with the simplification considering the bone to be homogeneous and linearly elastic, symmetric muscle action, complete osseointegration and static load [1,11,5,14,20]. Many of the options adopted in the current model should be taken into account in the analysis of results. Complete osseointegration is not observed in clinical studies, as the level of osseointegration is highly variable. In a 3D FE analysis of osseointegration percentages and patterns on implant-bone interfacial stresses, Papavasiliou et al. [21] concluded that different degrees of osseointegration do not affect the stress levels or distributions for axial or oblique loads. Therefore, fixing a value of 100% in a comparative study has no effect on the conclusions.

The consideration of an interface resistance limit between bone and implant not included in the model is an interesting topic to be included in future models, and requires a non-linear treatment of the problem considering contact and fracture at the implant bone boundary layer. In recent years, several studies have shown that a more precise consideration of the

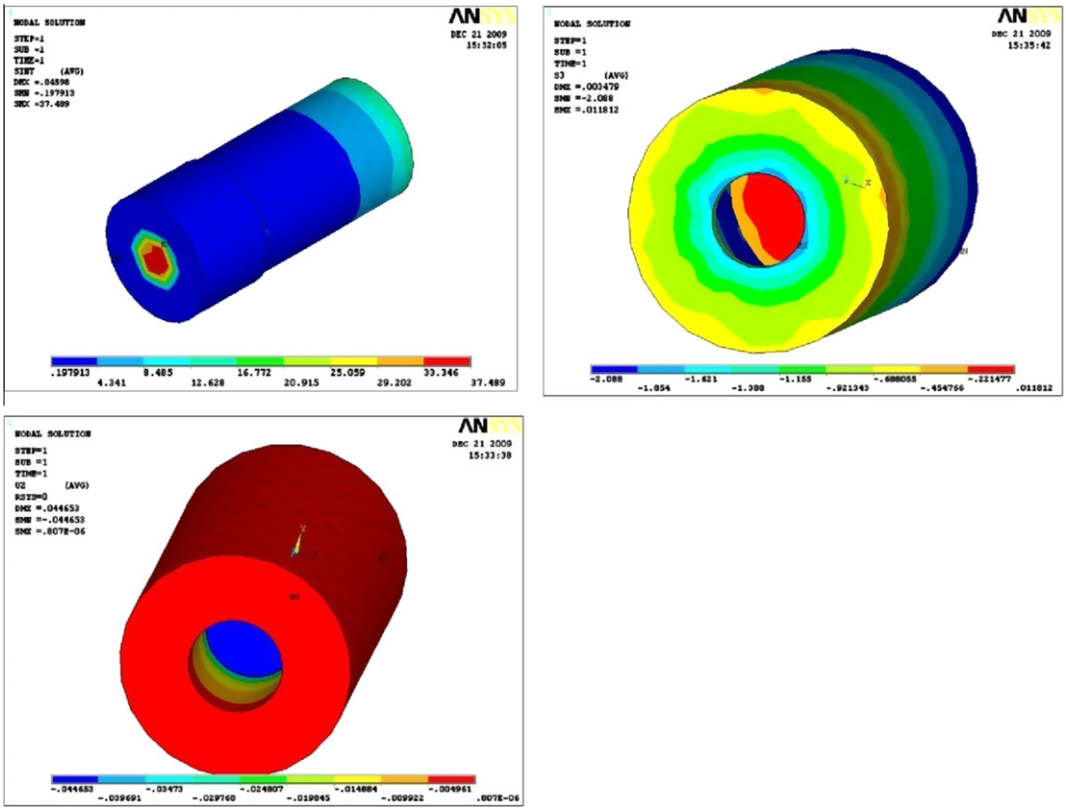

Figure 10 Sample of obtained results of model No. 25 under 50 N compressive loading (stress intensity on implant, maximum compressive stress on cortical bone, and vertical displacement in spongy bone).

physical processes in FE models used in dental biomechanics can lead to reliable results [3]. The modeling of whole mandible, the muscles, the temporomandibular joint and the supporting system, can bring the model closer to reality [6]. Three-dimensional modeling, special attention to boundary conditions, and the use of a fine mesh with appropriate number of degrees of freedom, are all factors that contribute to the precision of computational results [16].

Previous studies have shown that the modeled muscular force action at bone surface generates stresses as high as those obtained around the implant. This fact provides a qualitative way of comparing the obtained stress levels and suggests that modeling of the whole mandible is important and should not be neglected [6].

Comparative FEM stress analyses between different implant geometries or different implant prosthetic concepts under the same conditions have been previously reported [16,24]. Comparisons under different modeling conditions could serve as a reference, but do not provide conclusive proof. However, different studies have presented comparisons with the Brånemark system, which is used as a practical standard as it can provide predictable and thoroughly studied clinical results [27].

Simulation results considered functioning implants, modeling crestal bone loss after a healing and loading period. These results have also highlighted the influence of implant length and diameter on load transfer mechanisms. In agreement with the numerically experienced trend proposed by Himmlová et al. [15] and Bozkaya et al. [2], maximum implant diameter seems to affect stress peaks at the cortical bone not the trabecular region, while stress values and distribution at the cancellous bone implant interface are primarily influenced by implant length. Nevertheless, to control the risk of bone overload and improve implant biomechanical stress-based performance, numerical results from the current study suggest that, for short implants, implant diameter can be considered more effective design parameter than implant length. In this context, the results of this study may be considered as complementary to similar, previously published studies [15,23]. Due to the simplified and different geometrical models usually used in these studies, Himmlová et al. [15], Bozkaya et al. [2] and Saab et al. [23], quantitative comparisons cannot be made. Analogously, Carter's et al. [4] hypotheses regarding the influence of the strain level of the bone on hypertrophic responses or bone resorption cannot be directly verified in a quantitative sense. Numerical simulations have confirmed that the risk of bone overload essentially affects regions around the implant neck [20].

In the present study, for small implant diameter (range 3.5–4.5 mm), increasing implant length dramatically decrease maximum tensile stress generated in cortical bone under tension loading (Fig. 2), and increases in spongy bone (Fig. 3). The large diameter showed more stable behavior under tension loading, proving that implant diameter is the dominant factor not the implant length. Similar results can be found for small and large diameters as shown in Figs. 4 and 5.

Von Mises stresses in Fig. 6 showed similar changes with increasing implant diameter under bending loading. Fig. 7,

on the other hand, showed that Von Mises stresses under bending loading, appeared on spongy bone highly depend on implant diameter that reduces the ratio between side and cross-sectional areas. Finally, Figs. 8 and 9 show torsion loading results on cortical and spongy bones. Implants with large diameters are stable and others with small diameters can have better performance when increasing their length (side area).

Conclusion

Within the limitations of this study, numerical simulations showed that implant design, in terms of both implant diameter and length, crestal bone geometry and placement site affect the mechanisms of load transmission.

Stress distribution pattern did not change from one implant to the other even with changing implant diameter or length. Values of stresses may alter a lot in case of changing implant diameter and/or length. Wide implants (5–6 mm diameter) behavior was not noticeably affected when its length was increased. On the other hand, small diameter implant behaviors were dramatically enhanced by increasing implant length (side area). Therefore, implant length is the dominant parameter in case of using a small diameter implant.

References

[1] T. Baiamonte, M.F. Abbate, F. Pizzarello, J.L. Lozada, R. James, J. Oral Implantol. 22 (2) (1996) 104–110.
[2] D. Bozkaya, S. Muftu, A. Muftu, J. Prosthet. Dent. 92 (2004) 523–530.
[3] A. Çaglar, C. Aydin, J. Ozen, C. Yilmaz, T. Korkmaz, Int. J. Oral Maxillofac. Implants 21 (1) (2006) 36–44.
[4] D.R. Carter, M.C. Van Der Meulen, G.S. Beaupré, Bone 18 (1) (1996) 55–105.
[5] Y. Ciftci, S. Canay, Int. J. Prosthodont. 14 (5) (2001) 406–411.
[6] S.D. Cook, A.M. Weinstein, J.J. Klawitter, J. Dent. Res. 61 (1) (1982) 25–29.
[7] M. Cruz, Tri-Dimensional Stress Analysis Around a Cuneiform Implant by the Finite Element Method. Campinas, Brazil, M.DSci. Thesis (Dentistry), Camilo Castelo Branco University, 2001, 134p.
[8] M. Cruz, T. Wassal, E.M. Toledo, L.P.S. Barra, A.C.C. Lemonge, Int. J. Oral Maxillofac. Implants 18 (5) (2003) 675–684.
[9] M.I. El-Anwar, Simple Technique to Build Complex 3D Solid Models, 19th International Conference on Computer Theory and Applications (ICCTA 2009), Alexandria, Egypt, 2009.
[10] M. El-Zawahry, M. El-Anwar, A. Elragi, R. Jandali, MJNRC 8 (2) (2009) 23–27.
[11] J.P. Geng, W. Xu, K.B.C. Tan, G.R. Liu, J. Oral Implantol. 30 (2004) 223–233.
[12] J.P. Geng, K.B.C. Tan, G.-R. Liu, J. Prosthet. Dent. 85 (6) (2001) 585–598.
[13] J.P. Geng, K.B. Tan, G.R. Liu, J. Prosthet. Dent. 85 (2001) 585–598.
[14] A. Geramy, S.M. Morgano, J. Prosthet. Dent. 92 (5) (2004) 434–440.
[15] L. Himmlová, T. Dostálová, A. Kácovsky, S. Konvicková, J. Prosthet. Dent. 91 (2004) 20–25.
[16] E.P. Holmgren, R.J. Seckinger, L.M. Kilgren, F. Mante, J. Oral Implantol. 22 (2) (1998) 80–81.
[17] S. Ihde, T. Goldman, L. Himmlova, Z. Aleksic, Oral Surg. Oral Med. Oral Pathol. Oral Radiol. Endod. 106 (1) (2008) 39–48.
[18] S. Ihde, T. Goldman, L. Himmlova, Z. Aleksic, J. Kuzelka, Biomed. Pap. Med. Fac. Univ. Palacky Olomouc Czech Repub. 152 (1) (2008) 169–173.
[19] P. Kohnke, ANSYS Theory Reference Manual, Ansys Inc., 1994.
[20] Luigi Baggi, Ilaria Cappelloni, Michele Girolamo, Franco Maceri, Giuseppe Vairo, J. Prosthet. Dent. 100 (2008) 422–431.
[21] G. Papavasiliou, P. Kamposiora, S.C. Bayne, D.A. Felton, J. Dent. 25 (6) (1997) 485–491.
[22] C.S. Petrie, J.L. Williams, Clin. Oral Implants Res. 16 (2000) 486–494.
[23] X.E. Saab, J.A. Griggs, J.M. Powers, R.L. Engelmeier, J. Prosthet. Dent. 97 (2007) 85–92.
[24] T. Satoh, Y. Maeda, Y. Komiyama, Int. J. Oral Maxillofac. Implants 20 (4) (2005) 533–539.
[25] M. Sevimay, F. Turhan, M.A. Kiliçarslan, G. Eskitascioglu, J. Prosthet. Dent. 93 (2005) 227–234.
[26] Tomas Goldmanna, Stefan Ihdeb, Jiri Kuzelkaa, Lucie. Himmlovac, Czech Repub. 152 (2) (2008) 309–316.
[27] S. Yokoyama, N. Wakabayashi, M. Shiota, T. Ohyama, Int. J. Oral Maxillofac. Implants 20 (4) (2005) 578–583.